Effect of ceria on properties of yttrium-doped strontium titanate ceramics

Koutcheiko, Serguei; Yoo, Yeong; Petric, Anthony; Davidson, Isobel

Publisher's version / Version de l'éditeur:
https://doi.org/10.1016/j.ceramint.2004.12.009
Ceramics International, 32, pp. 67-72, 2005-03-05

ELSEVIER

Ceramics International 32 (2006) 67–72

CERAMICS INTERNATIONAL

www.elsevier.com/locate/ceramint

Effect of ceria on properties of yttrium-doped strontium titanate ceramics

Serguei Koutcheiko [a,*], Yeong Yoo [a], Anthony Petric [b], Isobel Davidson [a]

[a] *Institute for Chemical Process and Environmental Technology, National Research Council Canada, Ottawa, Canada K1A 0R6*
[b] *Department of Material Science and Engineering, McMaster University, Hamilton, Canada L8S 4L7*

Received 11 October 2004; received in revised form 3 December 2004; accepted 3 December 2004
Available online 5 March 2005

Abstract

This work reports the preparation and properties of the ceramic mixtures of the A-site deficient perovskite $Sr_{0.94}Y_{0.04}TiO_3$ (SYT) with CeO_2 in a range of ratios with a view to establishing their potential as anode materials for solid oxide fuel cells. Good electrical conductivity that decreased with increasing CeO_2 content was observed on reduction in forming gas. The composition with 50 wt.% of CeO_2 showed the conductivity of 7.0 S/cm at 900 °C in forming gas. The thermal expansion of SYT–CeO_2 ceramics in forming gas and in air were investigated in the range 25–900 °C at a ramping rate of 3 °C/min and thermal expansion coefficients were determined. The addition of ceria was found to have a positive influence on the catalytic behavior of SYT–CeO_2 ceramics towards steam methane reforming.

Keywords: A. Sintering; B. X-ray methods; C. Thermal properties; D. Perovskites

1. Introduction

The development of ceramic anodes for operation in methane is becoming an important task in SOFC development. The effective electrochemical reaction zone for conventional Ni/YSZ interface is limited to the area around the physical triple-phase boundary (TPB). The use of a mixed-conducting oxide as a porous anode is expected to enlarge the reaction zone to the entire electrode-gas interfacial area, which may lower polarization losses [1]. The electrical properties of oxides may be tailored by control of the composition and oxygen partial pressure [2]. This has been shown for fluorites, perovskites, and more complex structures [3–5]. The specific set of requirements which should be satisfied to optimize the behavior of oxide anodes includes good electronic and ionic conductivity, thermal stability over a rather wide range of oxygen partial pressure, sufficient catalytic activity, compatibility with solid electrolyte and other SOFC components, etc. [6]. There is evidence in the literature that ceria-based ceramics offer the dual benefits of conductivity and catalytic activity. Both doped and undoped ceria are mixed ionic and electronic conductors at low oxygen partial pressure. CeO_{2-x} has high values of oxygen surface exchange and diffusion coefficients and exhibits n-type conductivity with a value of 1 S/cm at 900 °C and at an oxygen partial pressure of 10^{-18} atm [7,8]. Failure to utilize the CeO_{2-x} electrode has been due to contraction of the lattice parameter causing mechanical cracking as the stoichiometry approaches a value of 2 when cycling to less reducing atmospheres. This problem can be minimized by using thin and porous electrode layers. Doping with lower valent cations is known to decrease the expansion and contraction of ceria during reduction and oxidation [9]. Another candidate material for anode applications is yttrium or rare earth-doped strontium titanate [10,11]. It was shown that $La_xSr_{1-x}TiO_3$ samples sintered in air exhibited relatively low electrical conductivities of 1–16 S/cm. However, $La_xSr_{1-x}TiO_3$ pre-treated in hydrogen at 1650 °C showed higher electrical conductivities, 80–360 S/cm, under the typical experimental conditions for SOFC anode operation [10]. Furthermore, these doped strontium titanate ceramics sintered on yttria-stabilized zirconia were found to be dimensionally and chemically stable when subjected to oxidation-reduction

* Corresponding author. Tel.: +1 613 993 2103.
E-mail address: serguei.koutcheiko@nrc.ca (S. Koutcheiko).

0272-8842/$30.00
doi:10.1016/j.ceramint.2004.12.009

cycling. However, the very low oxygen mobility observed in these titanates indicates that these compositions do not exhibit significant mixed conductivity [12]. To produce an effective and catalytically active anode material may, therefore, require the fabrication of a composite material with a good ionic conductor such as a stabilized zirconia or doped ceria. Recently, a novel (La,Sr)TiO_3–CeO_2 ceramic SOFC anode was developed [13]. These ceramics featured excellent electrocatalytic reactivity towards hydrogen at elevated temperatures and exhibited good compatibility with existing solid electrolytes. It was demonstrated that doped strontium titanate-based anodes are tolerant to sulfur-containing atmospheres.

The main goal of this work was fabrication of yttrium-doped strontium titanate ceramics mixed with CeO_2 and investigation of their electrical, mechanical, and catalytic properties.

2. Experimental

Ceramic samples of $Sr_{1-1.5x}Y_xTiO_3$, $x \leq 0.08$ were prepared by solid-state reaction. Dried $SrCO_3$ (purity 99.9%, Aldrich, Milwaukee, WI, USA), Y_2O_3 (purity 99.9%, Aldrich), and TiO_2 (purity 99.9%, Alfa Aesar, Ward Hill, MA) were mixed in a proper ratio, ground in a mortar with pestle, and calcined at 1200 °C for 5 h in air. Then the powder was reground, pressed into pellets, and sintered at 1380 °C for 5 h in forming gas (FG, 8% H_2 in Ar). The sintered disks were crushed and ball milled in ethanol. CeO_2 (purity 99.99%, Aldrich) and $Sr_{0.94}Y_{0.04}TiO_3$ (SYT) were used for mixture preparations. Three mixtures of SYT–$x$$CeO_2$, where x = 10, 30, 50 wt.% of CeO_2 were calcined at 1250 °C for 2 h in air. These ceramics were sintered in forming gas at 1300–1400 °C for 5 h. Relative densities of these SYT–$x$$CeO_2$ ceramics were 58, 65, and 70% for x = 10, 30, and 50 wt.%, respectively.

Diffraction patterns were obtained on powders and ceramics on a Bruker D8 Advanced X-ray diffractometer (Bruker AXS Gmbh, Karlsruhe, Germany) with Cu Kα radiation over the range of 2θ = 20–80°. For accurate lattice parameter determination, silicon was used as a standard. The unit cell parameters were derived from a computerized least-squares refinement technique.

Thermal expansion coefficients (TEC) were measured using a thermo mechanical analyzer (Setsys Evolution, Setaram, Caluire, France) in the temperature range from 25 to 950 °C in flowing forming gas or air (flowing rate 40 cm^3/min) with heating and cooling rates of 3 °C/min. The measurements were performed on small rectangular bars ~5 mm × 5 mm × 4 mm in accordance with ASTM standard E 831.

The conductivity was measured by a standard four-probe DC method. The samples were cut from the sintered bars with dimensions 16 mm (L), 3–5 mm (W), 3–4 mm (H). For the voltage contact, grooves, 0.10–0.15 mm deep, were cut approximately 3 mm from each end of the sample bar. Pt wire (0.127 mm diameter) was wound tightly into the grooves to form the potential probes. Pt mesh was attached to both ends of the sample by Pt paste 4082 (Ferro Electronic Materials, Vista, CA, USA). The contacts were cured in situ under forming gas for 1 h at 900 °C. A current of 80 mA from a Keithley 2400 current source (Keithley Instruments Inc., Cleveland, OH, USA) was passed through the sample and the voltage drop was recorded by a HP 3457A multimeter (Agilent Technologies, Palo Alto, CA, USA). The conductivity was measured in forming gas over the temperature range 600–900 °C.

The catalytic investigations were carried out in a small reactor (silica tube 4 mm inside diameter) with the charge of powder (0.3 g) mixed with silica fiber and positioned in the hot zone of a furnace. Measurements were made in flowing methane (5.5% in Ar) saturated with H_2O at 30 °C at a rate of 30 cm^3/min. The heating rate was 10 °C/min. Heating tapes were used to avoid water condensation and gas adsorption in the gas tubes. Product analysis was carried out with QME 200 mass spectrometer (Balzers, Hudson, NH, USA) calibrated for CH_4, Ar, CO, CO_2, H_2 with standard gas mixture. The powders were heated in situ at 1000 °C for 4 h in forming gas and cooled to 300 °C prior to the measurement. The temperature was maintained at this level in a flow of Ar prior to switching to the CH_4/H_2O/Ar mixture.

3. Results and discussion

3.1. XRD analysis

The solubility of Y^{3+} in $SrTiO_3$ is very limited. Single-phase samples were observed by powder X-ray diffraction

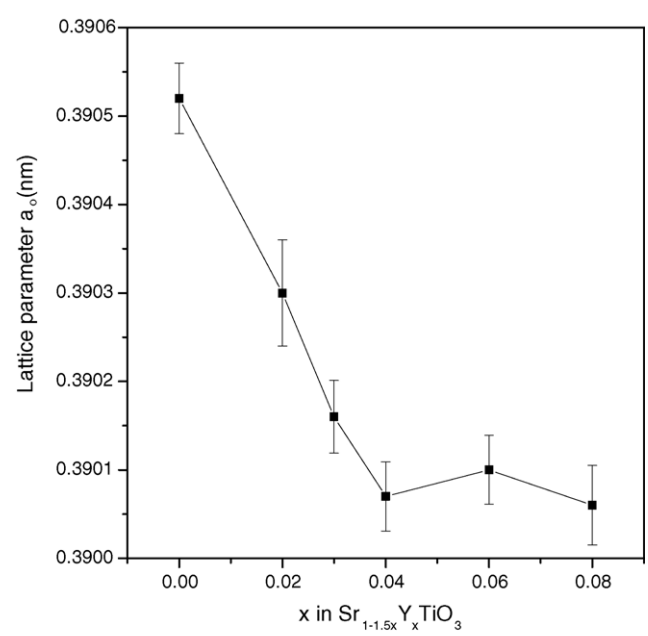

Fig. 1. Lattice parameter a_0 of $Sr_{1-1.5x}Y_xTiO_3$ phases as a function of x.

of $Sr_{1-1.5x}Y_xTiO_3$ for $0 \leq x < 0.04$. Sintering under reducing conditions didn't enhance the solubility range in this case [14]. When a single phase was present, its diffraction pattern resembled very closely that of cubic $SrTiO_3$. The resulting lattice parameters are shown in Fig. 1 as a function of composition. The lattice parameter decreased as the concentration of Y^{3+} increased to the point of Y^{3+} saturation, after which a_0 remained constant. Further increase of Y in the system resulted in formation of $Y_2Ti_2O_7$ and TiO_2. Traces (about 1% of the intensity of the strongest peak of perovskite phase) of the pyrochlore phase were observed in the XRD pattern of $Sr_{0.94}Y_{0.04}TiO_3$.

X-ray diffraction analysis of samples of SYT–xCeO$_2$, where x = 10, 30, 50 wt.% showed that they consisted of two phases, namely, perovskite "$SrTiO_3$-like" SYT and fluorite CeO_2. Fig. 2 shows the XRD pattern of a 50:50 (wt.%) mixture of SYT and CeO_2 powders prepared in air at 1300 °C for 2 h that is representative of this series. No pyrochlore phase was detected in the mixture. Lattice parameters were determined for perovskite and fluorite phases by indexing their diffraction peaks by analogy with those of $SrTiO_3$ and CeO_2, respectively. Cell parameters for SYT–CeO_2 samples prepared in air and forming gas at 1300 °C for 2 h are given in Table 1.

The data indicate that no reaction occurred between SYT and CeO_2. Cell parameters are very close to those reported for pure SYT (0.39007 nm, [15]) and CeO_2 (0.54109 nm, [16]) and independent of SYT/CeO_2 ratio. On reduction all samples exhibited an approximate expansion in unit-cell parameters of 0.05% and 0.23% for perovskite and fluorite phases, respectively.

Table 1
Lattice parameters for SYT–CeO_2 samples sintered in air and forming gas at 1300 °C for 2 h

CeO_2 (%)	a_0 for SYT ($\times 10^{-1}$ nm)		a_0 for CeO_2 ($\times 10^{-1}$ nm)	
	Air	FG	Air	FG
10	3.9003(6)	3.9018(4)	5.4101(6)	5.4217(9)
30	3.9001(7)	3.9020(9)	5.4106(8)	5.4228(6)
50	3.9004(9)	3.9022(8)	5.4100(5)	5.4230(9)

3.2. Conductivity

In Fig. 3 the temperature dependence of the conductivity of porous SYT–xCeO$_2$ ceramics in forming gas is shown as a function of CeO_2 content. It is clear that conductivity and activation energy decrease with increasing CeO_2 concentration. The electrical conductivity at 900 °C in forming gas was found to be 15.4, 9.3, and 7.0 S/cm for the samples with x = 10, 30, and 50%, respectively. The Arrhenius plots were not perfectly linear for the samples investigated. For simplicity, averaged activation energy values were derived from the Arrhenius plots in the range 650–800 °C.

3.3. Thermal expansion behavior

The thermal expansion behavior under reducing conditions of SYT–xCeO$_2$ sintered in forming gas at 1300 °C for 2 h is shown in Fig. 4. For comparison, the thermal expansion of yttria-stabilized zirconia (YSZ) sintered at 1400 °C in air was plotted as well. It was seen that thermal expansion coefficients (TEC) of SYT mixed with CeO_2 were higher than that of YSZ and increased with increasing ceria concentration. The thermal expansion of SYT–CeO_2

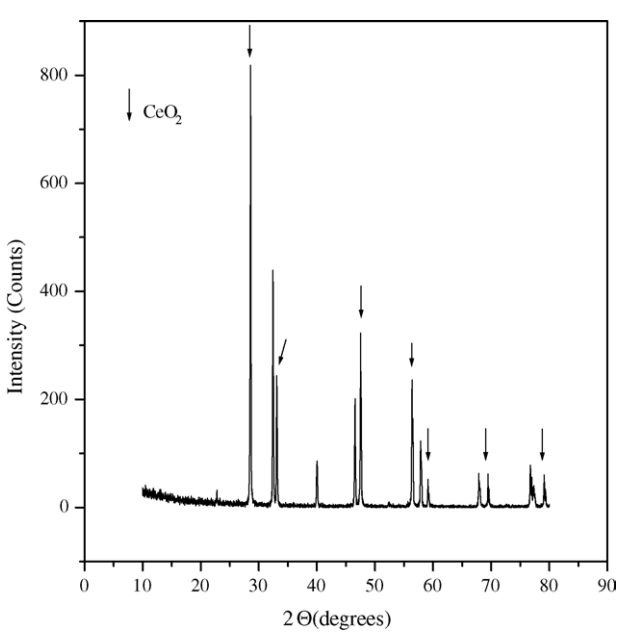

Fig. 2. XRD pattern for SYT–50CeO_2 heated in air at 1300 °C, 2 h.

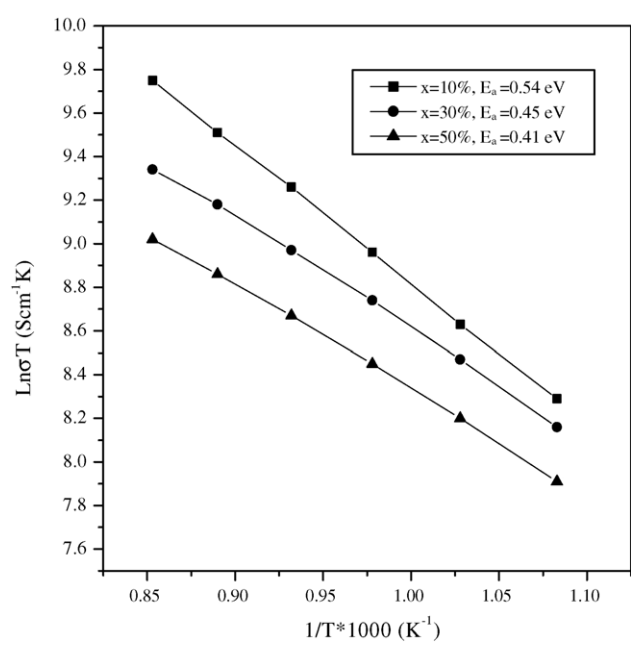

Fig. 3. Arrhenius plot of electrical conductivity of SYT–xCeO$_2$ ceramics, with x = 10, 30, 50 wt.% in forming gas.

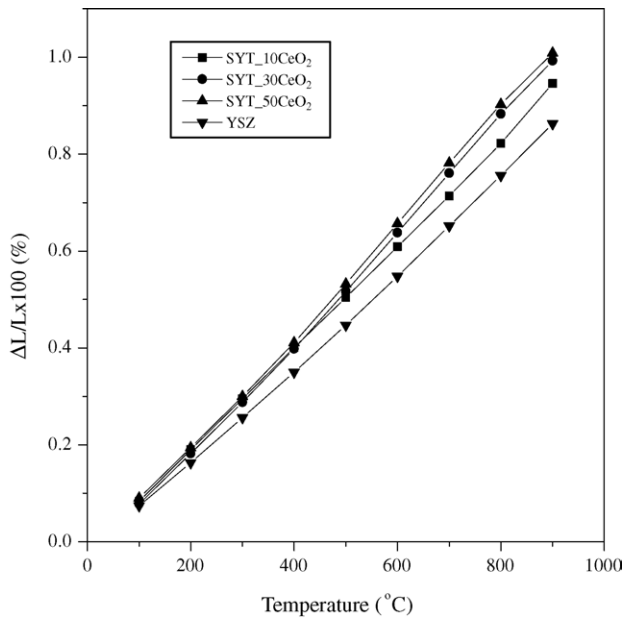

Fig. 4. Thermal expansion of reduced SYT–xCeO$_2$ ceramics in forming gas as a function of temperature.

materials increased almost linearly in the range 100–900 °C. The average thermal expansion coefficients calculated in the temperature range 400–900 °C were 10.9, 11.9, 12.3, and $10.3 \times 10^{-6}\,K^{-1}$ for $x = 10$, 30, 50, and pure YSZ, respectively.

Fig. 5 shows the expansion of reduced ceria-doped SYT ceramics heated in air. Three distinctive regions can be seen in the figure. Below 250 °C, $\Delta L/L$ only slightly increased with temperature. The thermal expansion coefficients in this region varied little with composition, but did increase slightly with increasing CeO$_2$ concentration and were found to be $10.6–11.2 \times 10^{-6}\,K^{-1}$. In the range 250–450 °C sample dimensions increased about 0.6–0.7% due to an oxidation process. Oxidized samples showed very similar TEC values in the range 500–900 °C. The experiment was repeated on fully oxidized samples at 900 °C. The average thermal expansion coefficients of oxidized materials in the temperature range 100–800 °C in air were 10.4, 10.5, $10.6 \times 10^{-6}\,K^{-1}$ for SYT–CeO$_2$ compositions with 10, 30, 50 wt.% of CeO$_2$, respectively. The average TEC of YSZ is approximately $10.3 \times 10^{-6}\,K^{-1}$ in the temperature range 50–1000 °C in air or H$_2$ atmosphere [17]. Therefore, a SYT–CeO$_2$ anode can be easily fabricated on the YSZ electrolyte surface in air due to the well-matched thermal expansion behavior. The effect of reduction–oxidation cycling on the relative expansion of SYT–50CeO$_2$ was studied (see Fig. 6). The reduced ceramic was rapidly heated (15 °C/min) up to 900 °C in forming gas. After equilibration, the atmosphere was changed to He and then to air. It was observed that exposure of the pre-reduced sample to air at 900 °C resulted in a rapid expansion of up to 0.15%. During cooling in air to 25 °C, the sample contracted almost 1% and then expanded by 1.1% during repeat heating in FG.

The results of TEC measurements showed that the oxidized SYT–CeO$_2$ ceramics had TECs that were close to that of the YSZ electrolyte. At the same time, the values observed under reducing conditions were critical. The materials can probably be used as thin porous anode layers in electrolyte supported SOFCs but their use for anode–supported cells is questionable. The difference in TEC of ceramic components may lead to delamination.

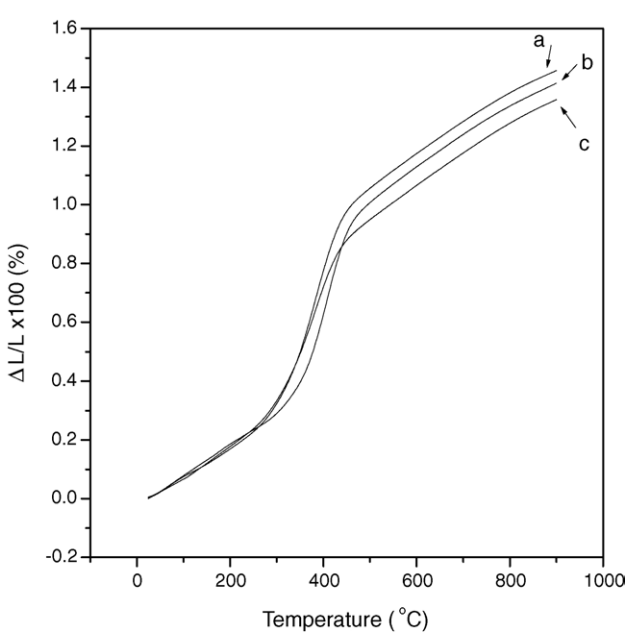

Fig. 5. Thermal expansion behaviors of reduced SYT–xCeO$_2$ ceramics in air as a function of temperature: (a) $x = 10$, (b) $x = 30$, (c) $x = 50$.

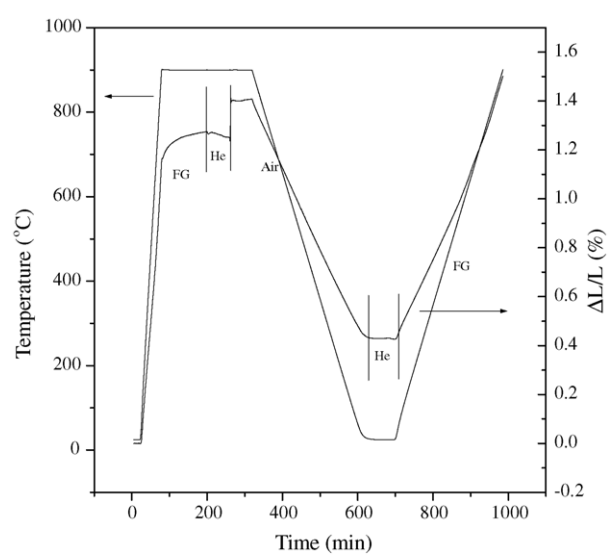

Fig. 6. Thermal expansion behavior of SYT–50CeO$_2$ ceramic during oxidation–reduction cycle.

3.4. Catalytic activity

Ordinary, methane highly diluted with inert gas like Ar does not undergo radical gas-phase decomposition. In order to determine the possibility of gas-phase methane cracking under our experimental conditions an initial test was carried out with a blank reactor in the temperature range 300–950 °C. There was no hydrogen detected below 950 °C. Our experiments showed that pure SYT was catalytically inactive in steam methane reforming. The temperature-programmed reactions of the pre-reduced SYT–xCeO$_2$ samples with moist CH$_4$ (5.5% balanced with Ar) gave rise to relatively simple spectra. The results of the measurement for SYT–50CeO$_2$ over the temperature range 300–950 °C are shown in Fig. 7. Below 750 °C no chemical reaction was observed and methane concentration remained constant (~5.5%). The main reaction involved the consumption of methane and water and the production of a large amount of H$_2$, some CO and some CO$_2$. Reaction products were detected above 750 °C and their concentrations gradually increased with temperature. At the same time the methane concentration decreased. Of course, complete conversion under these experimental conditions was not expected. It is known that reactive oxygen species can be formed in pre-oxidation processes, must be destroyed during pre-reduction and therefore cannot be formed by exposing the pre-reduced material to water [18]. Probably, the whole process can be attributed to a combination of the steam reforming of methane (1) and gas shift reaction (2):

$$CH_4 + H_2O \leftrightarrow CO + 3H_2 \quad (1)$$

$$xCO + xH_2O \leftrightarrow xCO_2 + xH_2 \quad (2)$$

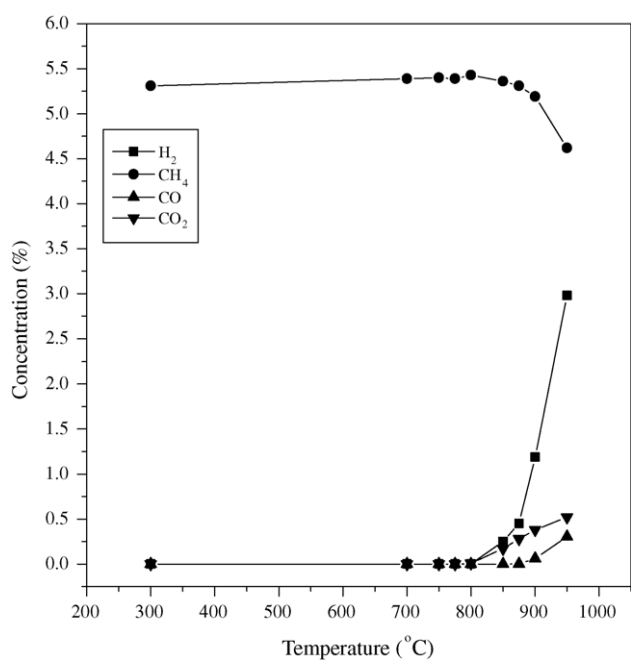

Fig. 7. Product distribution in temperature-programmed reaction of CH$_4$ with H$_2$O on SYT–50CeO$_2$ catalyst.

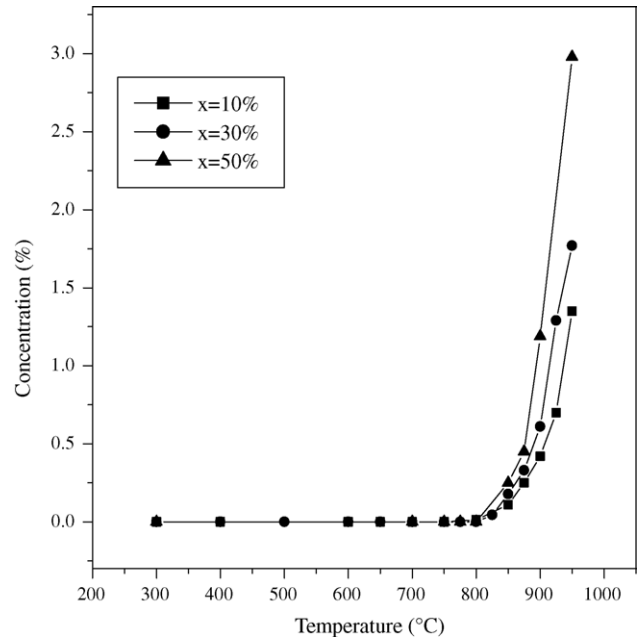

Fig. 8. Temperature dependence of H$_2$ formation during methane reforming on SYT–xCeO$_2$ catalysts.

and the addition of (1) and (2) gives,

$$CH_4 + (1+x)H_2O \leftrightarrow (1-x)CO + xCO_2 + (3+x)H_2$$

The inspection of the catalyst after the measurement of catalytic activity did not reveal any carbon that could have occurred from methane cracking (3):

$$CH_4 \rightarrow C + 2H_2 \quad (3)$$

Therefore, the catalytic activity of SYT–CeO$_2$ ceramics to methane cracking is suppressed. It was found that the catalytic activity of SYT–CeO$_2$ depends on CeO$_2$ concentration. The highest catalytic activity was observed for the sample with 50% of CeO$_2$. The amount of reaction products, H$_2$, CO, CO$_2$, increased with increase of CeO$_2$ concentration. For example, the amount of H$_2$ was 1.4, 1.9, and 3.0% for materials containing 10, 30, and 50% of CeO$_2$, respectively (see Fig. 8). Thus, CeO$_2$ increased the catalytic activity of the SYT–CeO$_2$ system towards methane reforming. This material revealed itself to be resistant to carbon deposition. To understand the role of CeO$_2$, further experiments are needed. It is possible that pure SYT can reveal catalytic activity being supported on CeO$_2$. On the other hand, ceria is also known to show high catalytic activity in redox reactions including methane and CO oxidation [19–21].

4. Conclusions

Thermal, electrical, and catalytic properties of $Sr_{0.94}Y_{0.04}TiO_3$–xCeO$_2$ (x = 10, 30, 50 wt.%) ceramics were studied in relation to their potential use as solid oxide fuel

cell anode materials. The samples sintered in forming gas exhibited an electrical conductivity on the order 7–15 S/cm at 900 °C, which is lower than the desired value for the anode. At the same time, their catalytic activity towards steam methane reforming was remarkably improved with the increase of CeO_2 content in the mixture. The oxidized samples prepared in air revealed TECs of 10.4–$10.6 \times 10^{-6}\,K^{-1}$ in air, which are very close to that of the YSZ electrolyte. Reduced samples exhibited 10.9–$12.3 \times 10^{-6}\,K^{-1}$ under forming gas atmosphere. SYT–CeO_2 ceramics sintered under reducing atmosphere were found to be dimensionally stable when subjected to oxidation-reduction cycling. The material containing 50 wt.% of CeO_2 showed only 0.15% expansion at 900 °C when forming gas was substituted by air. In view of the thermal expansion matching, catalytic activity and high temperature conductivities, the composition of SYT with 30 wt.% CeO_2 can be considered as a potential component for SOFC anode.

Acknowledgements

This work was supported by the Natural Sciences and Engineering Research Council of Canada (NSERC). The authors would like to acknowledge P.C. L'Abbe for technical assistance.

References

[1] T. Takahashi, H. Iwahara, I. Ito, Solid solutions of ceria as an anode material for solid electrolyte fuel cells, Denki Kagaku 38 (1970) 509–513.

[2] H.L. Tuller, Semiconduction and mixed ionic-electronic conduction in nonstoichiometric oxides: impact and control, Solid State Ionics 94 (1997) 63–74.

[3] O. Porat, M.A. Spears, C. Heremans, I. Kosacki, H.L. Tuller, Modeling and characterization of mixed ionic-electronic conduction in $Gd_2(Ti_{1-x}Mn_x)_2O_{7+y}$, Solid State Ionics 86–88 (1996) 285–288.

[4] P. Holtappels, J. Bradley, J.T.S. Irvine, A. Kaiser, M. Mogensen, Electrochemical characterization of ceramic SOFC anodes, J. Electrochem. Soc. 148 (8) (2001) 923–929.

[5] P.R. Slater, J.T.S. Irvine, Niobium based tetragonal tungsten bronzes as potential anodes for solid oxide fuel cells: synthesis and electrical characterization, Solid State Ionics 120 (1999) 125–134.

[6] B.C.H. Steele, P.H. Middleton, R.A. Rudkin, Material science aspects of SOFC technology with special reference to anode development, Solid State Ionics 40/41 (1990) 388–393.

[7] B.C.H. Steele, J.M. Floyd, The oxygen self-diffusion and electrical transport propeties of non-stoichiometric ceria and ceria solutions, Proc. Br. Ceram. Soc. 19 (1971) 55–76.

[8] H.L. Tuller, A.S. Nowick, Defect structure and electrical properties of nonstoichiometric CeO_2 single crystals, J. Electrochem. Soc. 126 (1979) 209–217.

[9] M. Mogensen, T. Lindegaard, U.R. Hansen, G. Mogensen, Physical properties of mixed conductor solid oxide fuel cell anodes of doped CeO_2, J. Electrochem. Soc. 141 (1994) 2122–2128.

[10] O.A. Marina, N.L. Canfield, J.W. Stevenson, Thermal electrical, and electrocatalytic properties of lanthanum-doped strontium titanate, Solid State Ionics 149 (2002) 21–28.

[11] S. Hui, A. Petric, Electrical properties of yttrium-doped strontium titanate under reducing conditions, J. Electrochem. Soc. 149 (1) (2002) J1–J10.

[12] P.R. Slater, D.P. Fagg, J.T.S. Irvine, Synthesis and electrical characterisation of doped perovskite titanates as potential anode materials for solid oxide fuel cells, J. Mater. Chem. 7 (12) (1997) 2495–2498.

[13] O.A. Marina, L.R. Pederson, Novel ceramic anodes for SOFCs tolerant to oxygen, carbon and sulfur, in: J. Huijsmans (Ed.), Proceedings of the Fifth European SOFC Forum, vol. 1, Lucerne, Switzerland, 2002, pp. 481–499.

[14] M. Abe, K. Uchino, X-ray study of the deficient perovskite $La_{2/3}TiO_3$, Mater. Res. Bull. 9 (1974) 147–156.

[15] S. Koutcheiko, Y. Yoo, A. Petric, Characterization of Y- and Nb-doped $SrTiO_3$ as a mixed conducting anode for solid oxide fuel cells, in: J. Huijsmans (Ed.), Proceedings of the Fifth European SOFC Forum, vol. 2, Lucerne, Switzerland, 2002, pp. 655–662.

[16] International Center for Diffraction Data, file 78-0694.

[17] M. Mori, Y. Hiei, N.M. Sammes, G.A. Tompsett, Thermal-expansion behaviors and mechanisms for Ca- or Sr-doped lanthanum manganite perovskites under oxidizing atmospheres, J. Elecrtochem. Soc. 147 (4) (2000) 1295–1302.

[18] R.T. Baker, I.S. Metcalfe, Activity and deactivation of $La_{0.8}Ca_{0.2}CrO_3$ in dry methane using temperature-programmed techniques, Appl. Catal. A: Gen. 126 (1995) 297–317.

[19] R.A. Tschope, W. Liu, M. Flytzani-Stephanopoulos, J.Y. Ying, Redox activity of nonstoichiometric cerium oxide-based nanocrystalline catalysts, J. Catal. 157 (1995) 42–50.

[20] K. Oitsuka, M. Hatano, A. Morikawa, Hydrogen from water by reduced cerium oxide, J. Catal. 79 (1983) 493–496.

[21] T. Bunluesin, R.J. Gorte, G.W. Craham, Studies of the water-gas-shift reaction on ceria-supported Pt, Pd and Rh: implications for oxygen-storage properties, Appl. Catal. B15 (1) (1998) 107–114.